JOURNAL OF GEOPHYSICAL RESEARCH, VOL. 91, NO. D8, PAGES 8672-8682, JULY 20, 1986

The Mg 280-nm Doublet as a Monitor of Changes in Solar Ultraviolet Irradiance

DONALD F. HEATH

Laboratory for Atmospheres, NASA Goddard Space Flight Center, Greenbelt, Maryland

BARRY M. SCHLESINGER

SASC Technologies, Incorporated, Hyattsville, Maryland

Five years of 160- to 400-nm solar flux measurements by the Solar Backscattered Ultraviolet experiment on Nimbus 7 have been analyzed. The flux in the center of strong lines and at shorter wavelengths varies with periods that correspond to modulation by the rotation of active regions. The modulation is greater at the centers of strong lines and at shorter wavelengths, corresponding to radiation that originates at higher levels in the solar atmosphere. The ratio of the irradiance in the core of the Mg 280-nm line to the irradiance at neighboring wavelengths is used as an index of solar variation. A scaling factor is derived by comparing rotational modulation at other wavelengths with the rotational modulation of the index. The scaled Mg II 280-nm strength successfully represents both rotational and long-term variations across the Al absorption edge near 210 nm. This ratio can therefore provide an empirical representation of long-term ultraviolet solar variability. Scaling factors are derived and changes estimated at several ultraviolet wavelengths. At 204 nm, in the wavelength region that drives atmospheric photochemistry, the solar irradiance drops about 4% from its average level for 1979–1980 to late 1983. The total estimated range of variation of the 27-day averaged (one rotation) 204-nm irradiance is 6%, over the 5 years of measurements. A least squares fit shows that over the 5 years, 27-day averages of 10.7-cm radio flux and of the Mg II index follow a linear relation. The radio flux can therefore be used to estimate changes in the solar ultraviolet for times before the launch of Nimbus 7.

1. INTRODUCTION

Solar ultraviolet radiation at wavelengths from 170 to 300 nm is a driver of the photochemistry of the middle atmosphere. In recent years, evidence has been accumulating that variations in solar radiation at these wavelengths could lead to changes in the physical processes and chemical balance of the middle atmosphere [*Brasseur and Solomon*, 1984] and in the overall global climate [*National Academy of Sciences*, 1982].

In general, two techniques have been used to measure changes in the ultraviolet solar flux: continuous monitoring by a single space-borne instrument and comparison of measurements at different times from balloon and rocket platforms. However, instrument calibration problems complicate both techniques. For continuous monitoring by a single instrument the instrument characteristics may change with time [e.g., *Heath*, 1980]. Changes in the signal resulting from changes in the instrument must then be separated from those arising from actual variations in the sun. For repeated measurements on separate flights the instruments must be intercalibrated. *Mount and Rottman* [1983*a*, *b*] have measured the solar spectrum from 180 to 310 nm with instruments aboard several rocket flights, but their quoted errors are on the order of 10%, larger than the anticipated changes in solar irradiance, especially at the longer wavelengths.

While changes in instrument sensitivity complicate determination of long-term solar changes from space-borne monitoring, measurements of short-term changes are less likely to be affected. *Heath* [1980] has reported on periodic variations of the solar flux in the 160- to 400-nm wavelength range from measurements by the Solar Backscattered Ultraviolet (SBUV) experiment on Nimbus 7. The periods, about 27 or 13.5 days, are consistent with those expected from modulation at the period of solar rotation. Measurements from the Solar Mesospheric Explorer [*Rottman et al.*, 1982; *Rottman*, 1983; *London et al.*, 1984] have revealed periodic solar variability in the range of wavelengths 120–300 nm. The evidence for solar variability has been reviewed in detail by *Newkirk* [1983], *Simon* [1981], and *Simon and Brasseur* [1983].

Radiation from wavelengths near the center of strong absorption lines at longer wavelengths originates at levels in the solar atmosphere comparable to those giving rise to the continuum near 200 nm. *Bumba and Ružičková-Topolová* [1967] discovered that emission at the core of the Ca II *K* line varied over periods comparable to that of the solar rotation. *White and Livingston* [1981] investigated the variations of the central 1 Å of the *K* line and demonstrated that these variations could be identified with the rotation of plage areas onto and around the visible hemisphere from limb to center and back to limb. Rotational modulation of the Ca II *K* line has been observed in other stars as well. *Wilson* [1978] observed short-term variability in the central 1 Å of the *H* and *K* lines in a number of stars but, because the time interval between measurements was too long, was unable to determine a period. *Vaughan et al.* [1981] carried out a program of daily observations of a number of stars and were able to identify the variations as rotational modulation. Since the stars observed by Wilson to vary over the short term also showed evidence of variations over periods comparable to a solar cycle, it would appear that the short-term variation and long-term behavior may share a common origin.

Because line centers and ultraviolet solar flux show similar modulation, line indices representing core variations may prove to be useful predictors of solar variability at other wave-

Paper number 6D0187.
0148-0227/86/006D-0187$05.00

lengths. *Lean et al.* [1982] and *Skumanich et al.* [1984] have used observations of the *K* line to develop a three-component model consisting of plage, network, and quiet sun components. This model has been used to investigate variations of solar 200- to 300-nm flux [*Lean*, 1984], Lyman α [*Lean and Skumanich*, 1983], and 10.7-cm solar radio flux [*Donnelly et al.*, 1983]. The model successfully predicts the time dependence of the solar ultraviolet irradiance over periods of several months in some detail; however, Donnelly et al. note that the time dependence over the 27-day rotation period differs between 10.7 cm and the solar ultraviolet, a result they attribute to changes with height in the solar atmosphere of center-to-limb variability. Before a line can be used to predict ultraviolet solar variability, it must be shown to exhibit solar modulation. *Livingston and Holweger* [1982] found none in an investigation of six visible lines and one infrared line formed in the photosphere. Selection of the line or lines to be used and, in a broad line, the particular wavelengths, must be based on an actual examination of rotational modulation.

Five years of measurements of the solar flux from the Nimbus 7 SBUV experiment, covering the wavelength range 160–400 nm, are now available. This wavelength range includes the Ca II *H* and *K* doublet, the Mg II *h* and *k* doublet, and the continuum wavelengths near 200 nm, those likely to drive atmospheric photochemistry. The data provide a useful base for investigating the use of variations in the cores of strong lines to monitor the ultraviolet solar irradiance. By comparing irradiances at line center to those at nearby wavelengths on either side of the line, the effects of instrumental change can be almost entirely eliminated. If this instrument drift is wavelength independent or the variation with wavelength is sufficiently slow to permit a linear representation, it will cancel in these ratios.

Section 2 provides a brief description of the instrument and the schedule of measurements. Section 3 analyzes the evidence for rotational modulation and shows that changes in the Mg 280 doublet can provide an empirical model for changes in the irradiance at shorter wavelengths. Section 4 shows that this model successfully estimates changes in the short-wavelength irradiance over the 5 years of measurements and presents a method that may be used to apply it to estimating changes in the solar irradiance at earlier times.

2. MEASUREMENTS

The solar irradiance measurements discussed in this paper were made with the SBUV instrument aboard the Nimbus 7 satellite. The satellite was launched in October 1978; measurements of solar flux began on November 7, 1978, and are continuing as of this writing (summer 1985). The satellite is in a sun-synchronous orbit that crosses the equator at local noon and midnight. The instrument is a tandem Ebert-Fastie double monochromator. The slit function is approximately triangular about maximum, with a width of 1.1 nm between the half-maximum points.

To measure the solar flux, a ground aluminum diffuser plate is deployed to reflect sunlight into the instrument. When the plate is not deployed, the satellite measures radiation reflected from the earth's atmosphere. For continuous scan measurements of the solar spectrum the instrument takes readings at intervals of 0.2 nm as it scans the region from 160 to 400 nm. *Heath et al.* [1975] describe the instrument in greater detail.

To calibrate the spectral radiometric sensitivity, standards of spectral irradiance obtained from the National Bureau of Standards illuminated the diffuser plate at a central distance of 50 cm. For wavelengths from 250 to 400 nm the laboratory irradiance calibration was based on measurements using 1000-watt tungsten-quartz-halogen FEL lamps; calibration for 200–250 nm was based on deuterium arcs, and calibration for 160–200 nm was based on an argon mini-arc. The FEL lamp calibration for 250–400 nm was the primary calibration. The deuterium arc calibration was normalized to the FEL lamp calibration by comparing measurements at wavelengths longward of 250 nm; the argon miniarc calibration for 160–200 nm was similarly normalized to the "corrected" deuterium arc calibration using measurements longward of 200 nm. The argon miniarc used for the calibration proved somewhat less stable than the deuterium arc and the uncertainty in the calibration constants derived from it were about 70% greater. Since the incoming signal shortward of 200 nm is appreciably weaker than the signal at longer wavelengths, the less accurate calibration and weaker signal make the measurements shortward of 200 nm noisier and less accurate than those at longer wavelengths. The calibrations for 200–400 nm were obtained in air at ambient temperature, while calibrations for 160–200 nm were made in an ion-pumped vacuum chamber at room temperature. The instrument sensitivity for angles other than those used in calibrating the spectral irradiance was measured independently at several wavelengths.

Solar flux measurements are generally made once a day, at the northern terminator. One measurement normally includes three scans. For two periods during the first 5 years the frequency of diffuser deployment for continuous scan solar flux measurement was increased from once per day to once during each of the 14 orbits per day: July 15 to November 18, 1980, and July 1 to September 17, 1981. During most of the 5 years, measurements were made on a cycle of 3 days on and 1 day off. Data gaps greater than 1 day are rare; none is greater than 3 days. The coverage in time is therefore sufficiently dense to permit a detailed study of the changes with time of solar irradiance over the 5 years. *Fleig et al.* [1983] discuss coverage and scheduling in greater detail.

The data have been corrected for instrument-related changes. Instrument measurements of calibration emission spectra from an on-board mercury lamp have shown that the wavelength corresponding to a particular scan position varies with time. The variation ranges from near zero at 160 nm to about 0.05 nm in 5 years at 400 nm. The variation is approximately linear with both wavelength and time. All irradiance time series in this paper are corrected to constant wavelength. Corrections have been applied for changes in the photomultiplier gain with time. These changes have been determined by comparing the photomultiplier signal with that from a reference vacuum photodiode having the same photocathode as the photomultiplier. In flight a beam splitter diverts a small part of the solar signal to the photodiode. Corrections have also been applied for the wavelength-dependent change in the reflectivity of the diffuser plate [*Park and Heath*, 1985]. There remains a wavelength-dependent change with time which is believed to be at least partly instrumental and has not removed from the data. It arises from a combination of effects not corrected for and from uncertainties in the other corrections. To eliminate the effects of this possible drift, the results of this paper are based only upon ratios of irradiances. Use of ratios eliminates wavelength-independent changes. If the wavelengths compared are reasonably close together, it also eliminates the wavelength-dependent effects, all of which vary slowly with wavelength. Instrument correction is discussed in

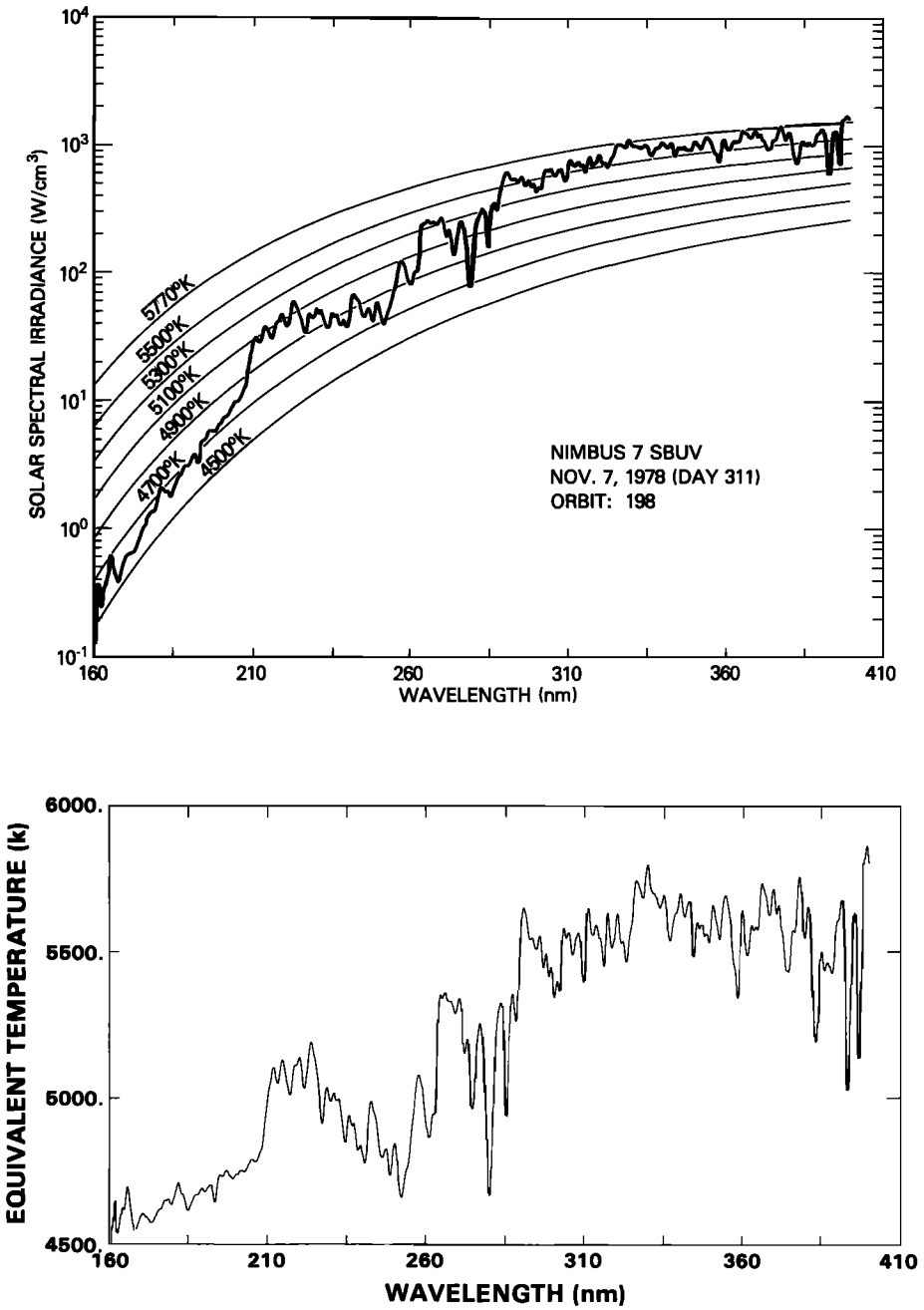

Fig. 1. (Top) Spectrum of solar irradiance, November 7, 1978, and (bottom) equivalent brightness temperature, same day.

more detail in the user's guides to the ozone products [*NASA*, 1984] and the continuous scan tapes (B. Schlesinger et al., unpublished manuscript, 1986.) A tape containing 5 years of continuous scan irradiance measurements has been archived at the National Space Sciences Data Center.

3. Rotational Modulation

The top panel of Figure 1 shows the measured irradiance as a function of wavelength for November 7, 1978. Because of the sharp decrease in irradiance with decreasing wavelength, spectral features are not clearly delineated at the shorter wavelengths. The features can be seen more easily by converting the irradiance to an equivalent brightness temperature. Lines of constant brightness temperature are shown along with the flux on the top panel, and brightness temperature as a function of wavelength appears in the bottom panel. When a Planck function appropriate to the gas kinetic temperature can describe the radiation field in the regions of origin of the measured flux, the brightness temperature serves as a guide to the temperature in those layers. In strong lines and at shorter wavelengths in the continuum, where radiative transfer departs from local thermodynamic equilibrium (LTE) processes, brightness temperature will not represent a physical temperature in the same way.

The plots show the principal solar spectral features for the wavelength range scanned: the Ca II *H* and *K* lines at 397 and 393 nm; the Mg I resonance line at 285.3 nm; the Mg II *h* and *k* doublet near 280 nm, which the instrument does not resolve; the Mg I and Al I ionization edges at 251 and 208 nm; the Si II emission line at 181.6 nm; and the C I line at 165.7 nm.

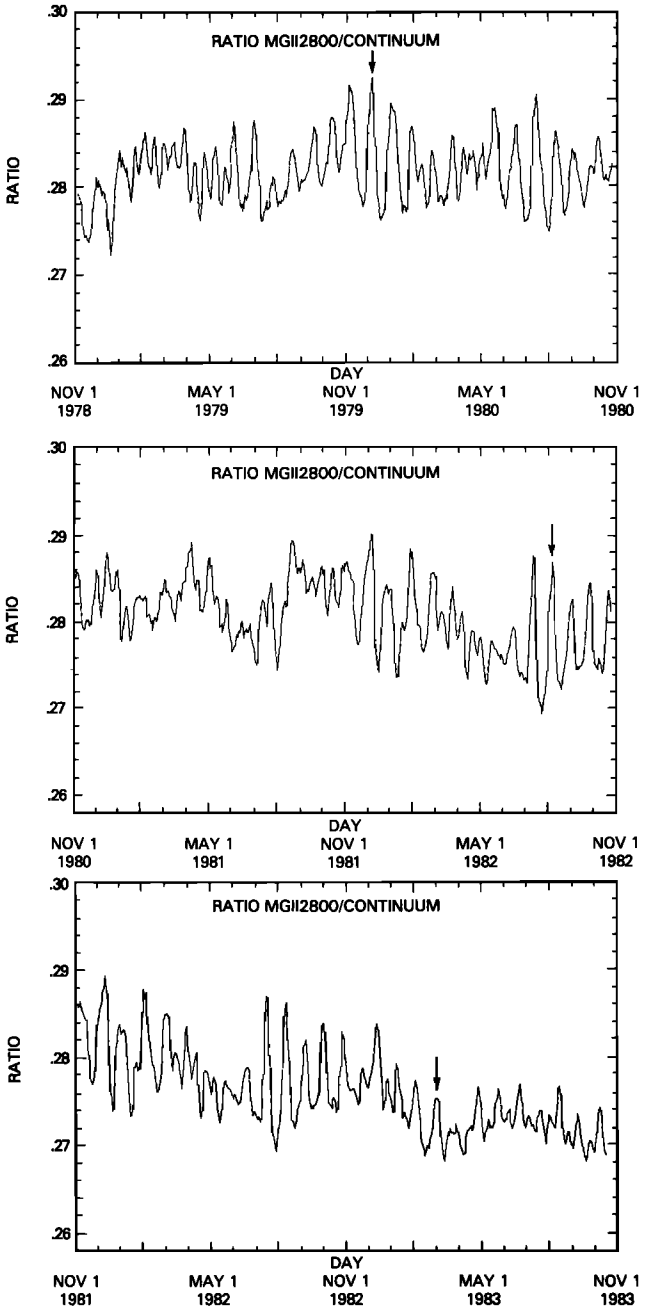

Fig. 2. Ratio of Mg II 280 nm to continuum: (top) November 1978 to November 1980, (middle) November 1980 to November 1982, and (bottom) November 1981 to November 1983.

Of the longer wavelength features the most conspicuous are the Ca II *H* and *K* lines, the Mg II *h* and *k* doublet, and a feature near 383 nm which is a blend of Mg I and Fe I lines and Balmer H9. At the band pass of the SBUV instrument the Mg doublet is not resolved, and the irradiances at both the Mg and Ca line center wavelengths include wing contributions of upper photospheric origin as well as core contributions of chromospheric origin. Because the Mg II line is stronger than Ca II *H* and *K*, it provides a better sample of the upper photosphere [*Morrison and Linsky*, 1978]. The brightness temperature at the center of the Mg doublet is closer to the brightness temperature at 200 nm than is that at any other longer wavelength, although because the core of the Mg doublet [e.g., *Milkey and Mihalas*, 1974; *Ayres and Linsky*, 1976] and possibly to some extent the continuum at 200 nm [*Vernazza et al.*, 1976] are not formed in LTE, the brightness temperature is not a strict representation of the level at which the radiation originates. However, because the measured irradiance at the center of the Mg doublet includes contributions from wavelengths well in the wings of the Mg line, where departures from LTE should be less important, the brightness temperature can be considered in choosing which line is most promising for further study. Variations in the unresolved Mg doublet were therefore examined first.

To eliminate the effect of wavelength-dependent instrument drift, the Mg doublet was represented by the ratio of irradiance near the center to the ratio from an interpolated near-continuum for the same wavelength. For the core, irradiances at 279.8, 280.0, and 280.2 nm were averaged. Because of the 1.1-nm band pass of the instrument this average includes significant contributions from wavelengths from 279.3 to 280.7

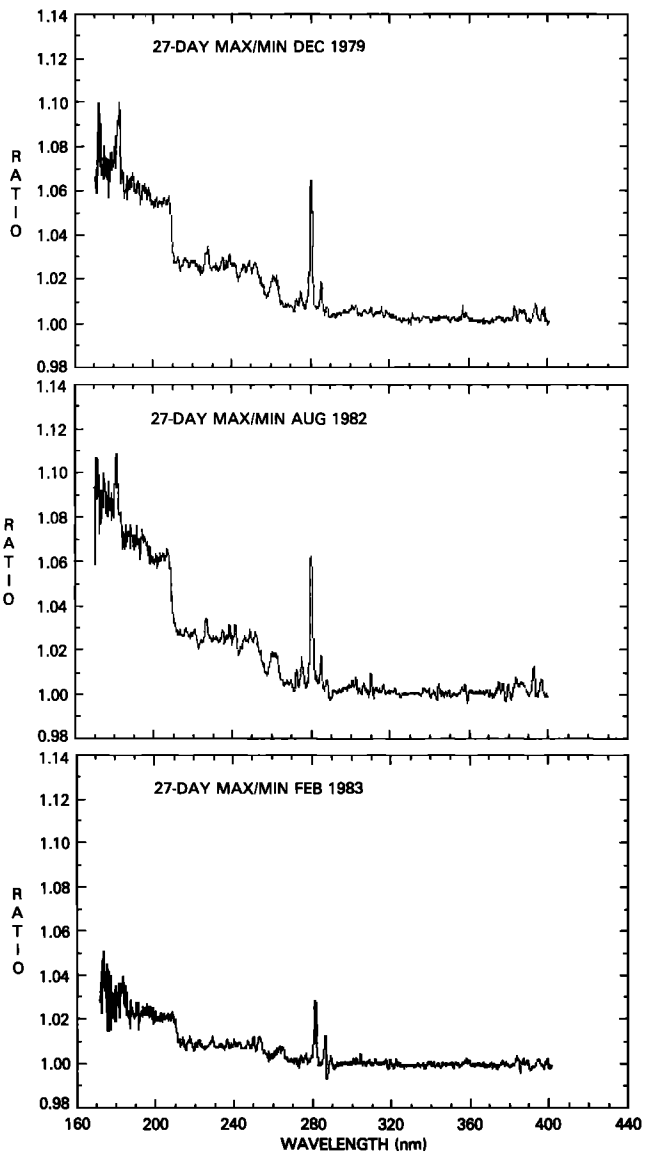

Fig. 3. Spectrum of ratio of maximum to minimum irradiance over a rotation, for the three rotations denoted by arrows in Figure 2: (top) December 1979; (middle) August 1982; and (bottom) February 1983.

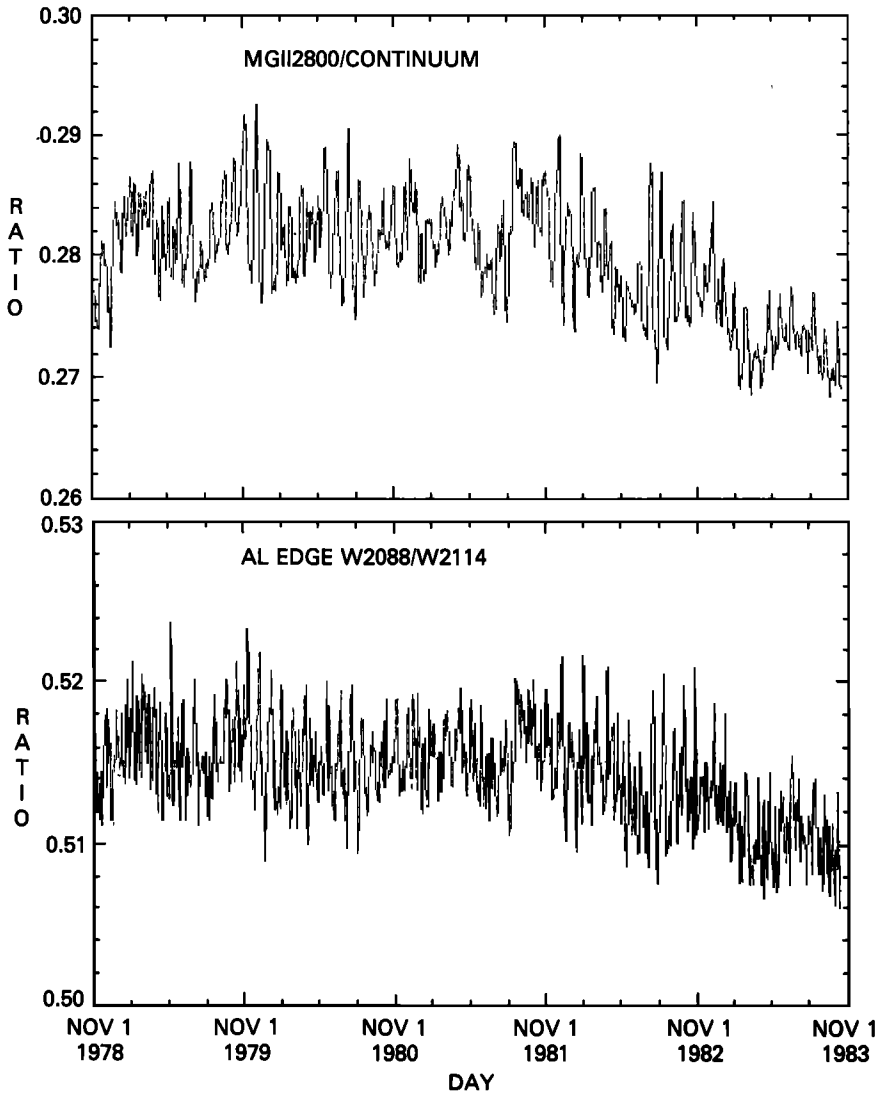

Fig. 4. Time dependence (top) of Mg II 280-nm core to continuum ratio and (bottom) of irradiance ratio across Al absorption edge.

nm, with the greatest weight from 279.7 to 280.3 nm. The interpolated near-continuum is derived by averaging irradiances at 276.6–276.8 and 283.2–283.4 nm, on both sides of 280 nm and equidistant from it. Both are at local maxima in measured irradiance as a function of wavelength and are therefore as close to the actual continuum near the Mg doublet as is likely to be attainable for the SBUV instrumental band pass. At 280 nm the rate of change of irradiance arising from instrument drift varies slowly with wavelength. Dividing the core irradiance by an average of wavelengths equidistant on either side will eliminate any residual wavelength dependence.

Figure 2 shows the time dependence of this Mg core index over the 5 years, 2 years at a time. The top panel shows the first 2 years of data, the middle panel shows the third and fourth year, and the bottom panel shows the fourth and fifth years. The overlap of the last 2 years allows clearer examination of the long-term changes, which are more pronounced in the later years. Several periods of strong variability with a period of approximately 27 days, corresponding to the effect of rotational modulation when active regions are clustered in one area of the sun, are present. The most conspicuous of these are centered in December 1979, July 1980, December 1981, August 1982, and February 1983. At other times, such as that centered around March 1979, active regions are in two groups of approximately equal strength on opposite sides of the sun, and the variability is regular, with a period of 13.5 days. At still other times, such as May 1983, the period of variability is 13.5 days, but the maxima are of unequal height, suggesting that the groups of active regions are of different strength. Rotational modulation of the solar flux is thus clearly present. This pattern of variation is not sensitive to position in the Mg line. The ratio of the average of irradiances at 278.6, 278.8, 281.0, and 281.2 nm to the same interpolated near-continuum showed the same features, although they were less clearly defined because the signal was weaker and the noise relatively stronger.

Figure 3 shows the wavelength dependence of the rotational modulation, comparing the irradiance at the Mg 280-nm maximum for a rotation with that at minimum. Results for three different rotations with strong modulation are shown, for times widely separated over the available period of data. These rotations are indicated by arrows on Figure 2. Each ratio compares the average for 3 days centered at cycle maximum to that for 4 days at surrounding minima, 2 days on

TABLE 1. Rotations Used for Scaling

Day of Maximum	Year
December 4	1978
January 13	1979
July 5	1979
October 17	1979
November 13	1979
December 12*	1979
January 6	1980
May 25	1980
June 23	1980
July 20	1980
August 16	1980
November 5	1980
January 31	1981
March 4	1981
December 9	1981
January 3	1982
February 2	1982
June 20	1982
July 17	1982
August 11*	1982
September 6	1982
October 1	1982
March 2	1983

*Period used in Figure 3.

either side. Use of minima both before and after eliminates almost entirely any effect on the derived ratios of decreases with time in the measured values due to instrumental changes. Clear increases of modulation with wavelength can be seen near the 208-nm aluminum edge and the Mg I ionization edge at 251 nm. Local modulation maxima occur at strong Fraunhofer lines: the Mg II 280-nm doublet, the Mg I line near 285 nm, and Ca II *H* and *K* lines at 397 and 393 nm. Comparison of Figures 1 and 3 shows that the magnitude of flux modulation over a rotation is directly related to the strength of the lines in a given wavelength region and that the degree of modulation increases overall with decreasing wavelength or increasing height in the solar atmosphere. This behavior probably arises from two sources: greater fractional area covered by active regions and stronger contrast between active regions and quiet sun at higher levels in the solar atmosphere [*Chapman*, 1981].

Figure 3 supports use of the Mg II doublet as the potential monitor of shorter wavelengths. At no other longer wavelengths, not at Ca II *H* and *K*, is the rotational modulation of irradiance integrated over the SBUV band pass comparable to that near 200 nm, a result which suggests that the solar layers contributing to the irradiance in the SBUV band pass near 280 may be more comparable to those contributing to the irradiance at shorter wavelengths than those responsible for the radiation elsewhere at long wavelengths. In addition, a wavelength with strong rotational modulation is desirable in order to maximize the signal-to-noise in the derived index. The origin of radiation measured near 280 nm is not identical to that for shorter wavelengths. Away from strong lines and absorption edges all radiation in the SBUV band pass should come from a limited height range in the solar atmosphere. In the Mg doublet, on the other hand, the irradiance over the band pass comes from a wide range of layers in the solar atmosphere. Departures from LTE in the formation of the Mg core could make its temporal variations different from those of radiation at shorter wavelengths, if radiation from different wavelengths with identical modulation in one rotation had appreciably different origins in the sun. The only way to determine whether a scaled Mg core index provides a satisfactory empirical model is to compare it with changes at shorter wavelengths.

While the suitability of the Mg index to represent shorter wavelengths over the short term could be evaluated using a single-wavelength band, evaluation of long-term behavior requires that a ratio be used, to eliminate wavelength-dependent instrumental changes. We have chosen to examine the time dependence of the irradiance ratio across the sharp change in solar flux seen in the SBUV measurements near the 207.6-nm Al edge. On each side of the edge the change with wavelength in level of origin of the radiation is small compared with the change across the edge.

Three-wavelength averages centered at 208.8 and 211.4 nm, 2.6 nm apart, were used. These two wavelengths mark the boundaries of the region where the solar flux changes most rapidly with wavelength. *Kjeldseth Moe and Milone* [1978] have noted that the Al edge solar flux break in Skylab measurements is longward of the laboratory wavelength; this behavior is also evident in the SBUV irradiance measurements. Unlike the situation near the Mg core, the difference in instrument degradation with time over the 2.6 nm is nonnegligible at the short wavelengths of the Al edge. To estimate this differential degradation, we calculated two sets of ratios of three-wavelength averages, 2.6 nm apart, on either side of the Al edge and equidistant from it: I(203.6 nm)/I(206.2 nm) and I(214.0 nm)/I(216.6 nm). In each case, $I(\lambda)$ represents a three-wavelength average of (λ, $\lambda \pm 0.2$ nm). Changes with time in these ratios combine effects due to instrument degradation with actual solar changes across 2.6 nm. Because the difference in observed rotational modulation between the two members of each of these pairs of wavelengths is small, particularly relative to the change near the Al edge, changes of the ratios with time should be dominated by degradation.

The differential degradation across 2.6 nm was taken to be the average of these two ratios. This average was divided out of the I(208.8 nm)/I(211.4 nm) Al edge ratio to remove differential instrument degradation.

Figure 4 compares the time dependence of the Mg II core to continuum ratio over 5 years with that of the resultant Al edge ratio. The Al edge ratio is considerably noisier. Still, at the time of strong 27-day variability in the Mg core the Al edge also shows strong 27-day variability. In addition, the long-term changes follow a similar pattern, with near constancy to late 1981, followed by a decrease. This similarity in changes with time suggests that the Mg core variations can serve as the basis of an empirical model for long-term variations in the 200–210 nm ultraviolet irradiance.

4. Long-Term Variations

The simplest way to use Mg core variations to represent shorter wavelengths is by scaling. Changes at shorter wavelengths are obtained by multiplying the Mg variations by a scale factor obtained from the ratio of the amplitudes of rotational modulation, comparing the modulation at short wavelengths with that at 280 nm. This approach can be tested by comparing the scaled Mg core variations with those actually measured in the 208.8/211.4 nm ratio, corrected for drift. The scale factor was derived using the calculated modulation for 23 rotations with strong 27-day irradiance variation. The variations over one rotation for both the Al edge, R(Al), and the Mg core, R(Mg), were calculated in the same way as the maxi-

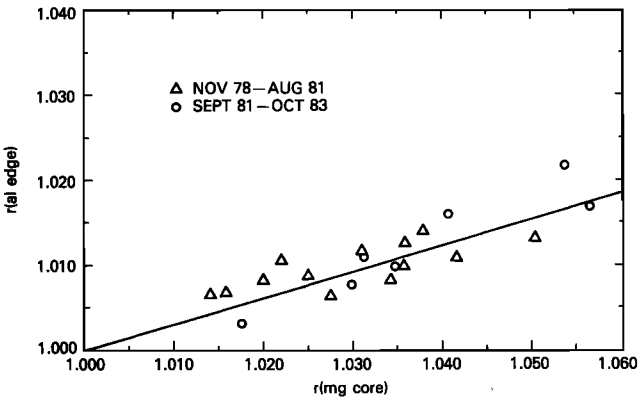

Fig. 5. Ratio of maximum to minimum irradiance for 23 rotations: Al edge vs. Mg II 280 nm. Triangles indicate rotations during November 1978 to August 1981; Circles show rotations during September 1981 to October 1983.

mum/minimum ratios for Figure 3, by taking the ratio of irradiance over 3 days centered at maximum to that at 4 days at surrounding minima, 2 day on each side. Table 1 lists the days of these maxima. The maxima shown in Figure 3 are marked with an asterisk. The separation between days of maximum for consecutive rotations may differ from 27 days because of off days or noise in the ratio. If the variations at 200 nm can be represented by a simple scaling of the Mg core variations, then the Al edge ratio would not vary when the Mg core does not vary. The 23 R(Al)/R(Mg) points derived from periods of strong modulation all represent appreciable departures from unity. Two points for R(Mg) = R(Al) = 1, that is, no variation, were added to the 23 rotations to represent periods of weak or absent variability. A linear least squares fit was then calculated to the points, yielding the scaling factor and the statistical uncertainty of the fit. In addition, scaling factors were derived from fits to more restricted periods of data. Differences between these fits and that for the entire period, as well as differences among the individual fits, were within the calculated statistical uncertainties of the scale factors. Figure 5 is a plot of Al edge maximum to minimum ratios against those for the Mg core for the 23 periods chosen for deriving the scaling factor. The straight line is the derived fit.

Examination of Figure 4 shows that the Mg core variations over the 5 years separate into two periods: the time through the major maximum of August 1981, when the variations are

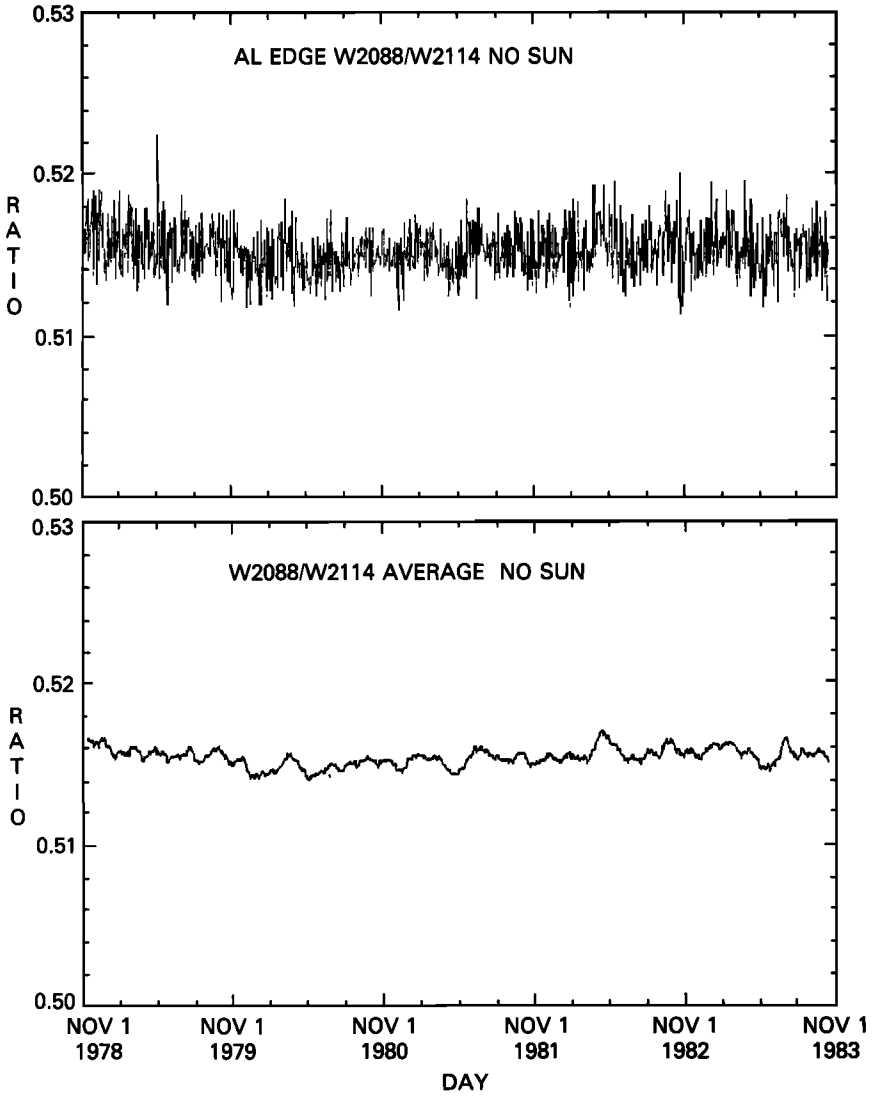

Fig. 6. Time dependence of residual Al edge ratio when solar change estimate from scaled Mg ratio has been removed: (top) daily values and (bottom) 27-day running average.

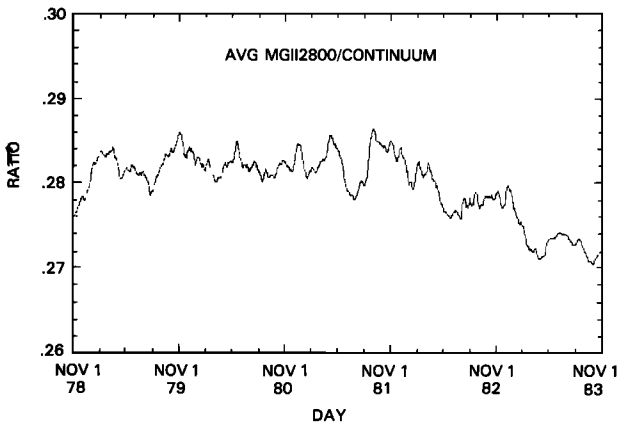

Fig. 7. Time of 27-day average Mg 280-nm core-to-continuum ratio.

about a consistent high level, and the subsequent period, during which there appears to be an overall decline in the Mg 280 irradiance coincident with the overall decline of solar activity from maximum. If the Mg ratio can successfully represent changes at shorter wavelengths, the relation between R(Mg) and R(Al) should be the same for both periods. Accordingly, different symbols have been used in the plot to represent the two periods: triangles for the period before and during the major maximum in August 1981 and circles for the later time.

The plot shows no systematic difference; the relation between the Al edge and Mg core ratios for individual rotations does not change systematically over the 5-year period of data. A single scaling factor represents the 5 years. The derived scaling factor, representing the ratio of the amplitude of flux variations in the ratio of the two wavelengths near the measured Al edge to that of the Mg 280 doublet index, is 0.31 ± 0.03.

To see more clearly how well the scaled Mg core index can model the changes at the Al edge, the scaled Mg core estimate for variations with time of the Al edge ratio were removed from the Al edge ratio, using the expression

$$I_{NS} = I_0/[1 + s(f - 1)] \quad (1)$$

where f is the Mg index ratio normalized such that the average over the first 13 Bartels periods (351 days) is unity, s is the scaling factor, I_0 is the Al edge ratio and I_{NS} the Al edge ratio with the estimated solar variability derived from the Mg index removed. In effect, (1) scales departures from some base value. The top panel of Figure 6 shows I_{NS} ("no sun" Al edge irradiance) as a function of time. Figure 6 shows no 27-day variability. The absence of 27-day variability in this time series has been confirmed by power spectrum calculations. There is also no systematic trend over the 5 years. There is some structure over periods of less than 27 days, but it is not clear whether it is pure noise or if there is some short-term periodicity. As noted earlier, the distribution of levels of origin in the sun for the irradiance in the Mg line differs from that for the irradiance detected near the Al edge. Consequently, as noted by *Donnelly et al.* [1983], differences in center-to-limb variability as a function of height in the solar atmosphere can produce a different shape for the 27-day variability. The long-term variability in the time series can be seen more clearly in a 27-day running average, which eliminates rotational modulation. The bottom panel of Figure 6 shows this average. Some structure with a duration of a few weeks to several months appears to be present; however, the only periodicity longer than 27 days evident in power spectrum and autocorrelation calculations is a maximum of about 0.2 in the autocorrelation, at 140 days. Whether these variations are linked to differences in the structure of different activity centers or are simply noise is not clear. A similar series was calculated by subtracting a scaled solar flux from the Si II 181.6-nm emission strength and calculating the 27-day average. The cross correlation between this Si II residual and the Al edge residual was calculated. If the structure were due to a physical property of the active regions, one would a expect a correlation, but the cross correlation was 0.0 to ± 0.02 for all lags, a result that suggests the residual in Figure 6 may be simply noise. The departure from a straight line of the residual is about 0.2% of the value of the Al edge ratio, or about 10% of the variability in the ratio, both over a 27-day cycle and over the entire period. The Mg core index provides an excellent representation of changes in the ultraviolet irradiance.

The long-term ultraviolet variability represented by the Mg line is clearer if the 27-day variability is removed. Figure 7 shows the 27-day average of the Mg core to continuum ratio. Wide peaks on the order of 6 months' duration correspond to the lifetimes of individual activity centers. Comparison with Figure 4 shows these maxima to coincide with periods of greatest rotational modulation. Superimposed on these variations is the previously noted overall decline beginning after the last major outburst of activity in late 1981. This change can be interpreted as a result of the decrease in the overall level of solar activity.

The method used to model long-term variations at the Al edge, scaling changes in the Mg core by the relative amplitude of 27-day variability, can be applied to irradiances at particular wavelengths as well as to wavelength ratios. Comparing the irradiance at the time of a maximum with that at surrounding minima when deriving scaling factors minimizes the effects of instrument sensitivity changes on the maximum-to-minimum ratio. Because they are derived from variations over a rotation, the scale factors have a wavelength dependence similar to that of the maximum-to-minimum ratios of Figure 3. Figure 7 can therefore be used as a guide to the wavelength

TABLE 2. Ultraviolet Solar Flux Variations

Wavelength	Scale Factor	Modeled Change, % (1979–1980 to 1983)	Modeled Range of 27-Day Average, %
Mg II core/continuum	1.00 (definition)	3.6 (actual)	5.7 (actual)
180.2 nm	1.49 ± 0.06	5.3	8.5
203.8 nm	1.04 ± 0.05	3.7	6.0
232.4 nm	0.44 ± 0.04	1.6	2.5
266.0 nm	0.09 ± 0.04	0.3	0.5

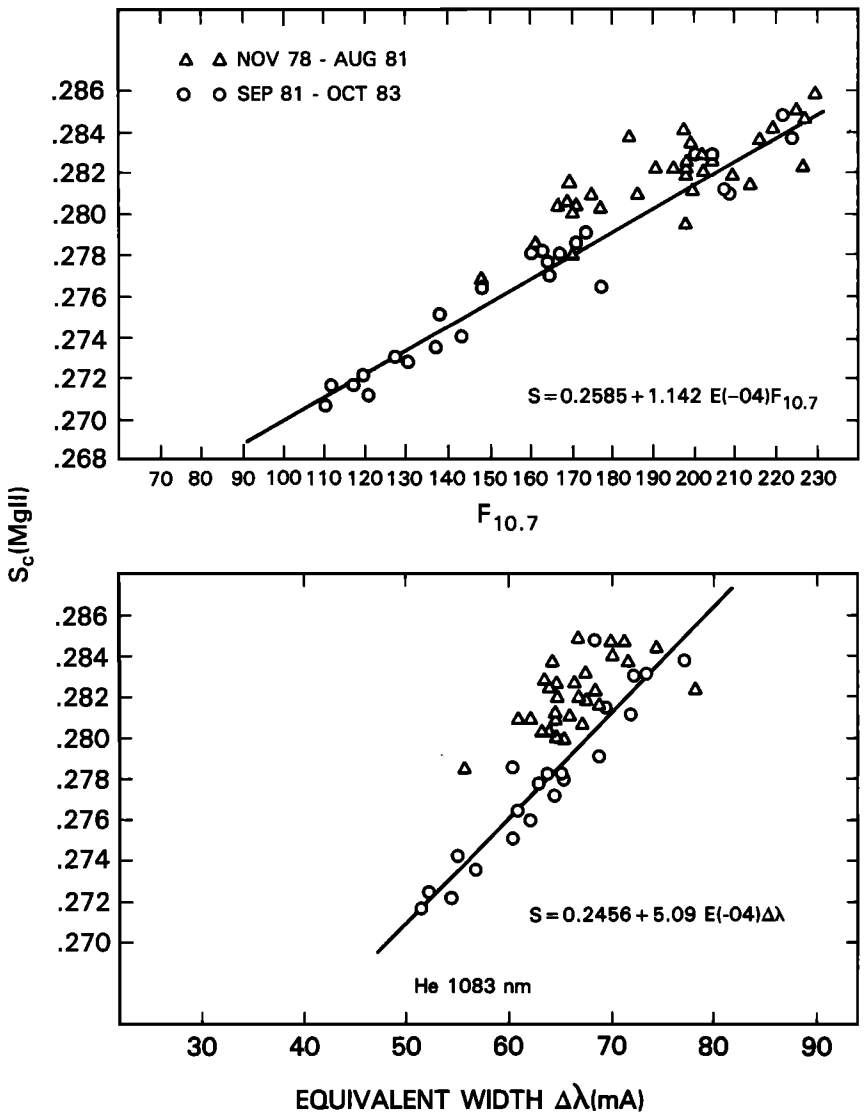

Fig. 8. Twenty-seven day average Mg II core to continuum ratio versus 27-day average He I 1083-nm width and monthly average 10.7-cm radio flux. Triangles represent period from November 1978 to August 1981; Circles indicate period from September 1981 to October 1983. Fit equation represents preliminary values, now superseded by Table 3.

dependence of long-term variability. To obtain variations at any wavelength, simply multiply by the difference from unity relative to that in the 280-nm doublet.

To see how the 5-year change varies with wavelength, calculations were carried out at four ultraviolet wavelengths: three to bracket the Mg and Al absorption edges and one as short as could be used before the scatter in the measurements became too large. All were chosen to be away from significant spectral features, the three longest at local maxima of irradiance for the SBUV band pass. To reduce the scatter, averages over five scan wavelengths were used. Table 2 shows the changes for the Mg II ratio, the scaling factors used to estimate the changes, and the modeled changes for the four wavelengths. The changes in the Mg ratio are based upon the 27-day averages shown in Figure 7. The first set (third column) is the change between the average solar flux for 1979–1980, the time of maximum, and the average over the last months of data in 1983. The second set (fourth column) contains the maximum amplitude of variation in the 27-day average over the 5-year period. The largest variations over a single rotation can be as great as the change in the 27-day average over the 5 years.

To investigate possibilities for modeling the UV solar flux outside the 5 years of SBUV data, correlations between the Mg core index and other indices of solar activity were examined. Values for Ca II plage indices are not available for a sufficient number of days to provide a complete distribution over most individual solar rotations. He I 1083-nm equivalent widths [*Harvey*, 1984], sunspot numbers, and $F_{10.7}$, the radio flux at 10.7 cm, were compared with the Mg core index. The daily spot numbers and values of $F_{10.7}$ were read from the "Magnetic Activity Tape," obtained from the National Space Sciences Data Center at NASA Goddard Space Flight Center. Averages over the 27-day Bartels periods 1986–2053, covering the period December 4, 1978, to October 16, 1983, were calculated for each of the indices. Linear fits for the 27-day average of each index as a function of that for the Mg index were calculated using the subroutine RLFOR of the *IMSL* [1982] software package. Table 3 lists the derived zero point and slope and the percentage standard error of each, the percent-

TABLE 3. Fits of 27-Day Average Solar Activity Indicator to Mg 280 nm

Indicator	Zero point		Slope		Percent of Variance Fit	Residuals From Fit
	Value	Error, %	Value	Error, %		
$F_{10.7}$	0.2594	0.4	1.13×10^{-4}	5.1	86	1.5×10^{-3}
Spot number	0.2672	0.3	9.61×10^{-5}	6.5	79	1.8×10^{-3}
He 1083 nm	0.2473	1.3	5.09×10^{-4}	10.0	68	2.0×10^{-3}

age of variation explained by the linear fit, and the standard deviation of residuals from the fit, as derived in the fitting process. In Figure 8 are shown in Bartels period averages for the Mg 280 index as a function of each of the others, along with the derived linear fit. Rotations before and during the last UV maximum are differentiated from those during the period of decline, as in Figure 5. Comparison of the plots shows that He I is significantly stronger relative to the fit for a given value of the Mg index during the later period. The values in Table 3 show that the fit to $F_{10.7}$ has a smaller standard error, explains more of the variance, and has a smaller standard deviation of residuals from the fit line than either of the other two fits. Variations in sunspot coverage have generally been linked to changes at visible rather than ultraviolet wavelengths [*Bruning and LaBonte*, 1983; *Donnelly et al.*, 1982].

Because the fit for 27-day averaged $F_{10.7}$ does not show a systematic difference between the early and late periods during the 5 years, it appears most suitable for extending the estimate of UV solar flux to longer period. The fit using the coefficients listed in Table 3 is given by the equation

$$S_c(\text{Mg II}) = 0.2594 + 1.143 \times 10^{-4} F_{10.7} \quad (2)$$

in which S_c(Mg II) is the Mg II core to continuum ratio. For periods outside the 5 years of SBUV measurements, $F_{10.7}$ measurements can be used to estimate the value that S_c would have, and then, using equations of the form of (1) and scaling factors such as those of Table 2, variations at individual ultraviolet wavelengths can be estimated for those periods. Solar variability over those longer periods will be the subject of a future paper.

5. Conclusions

We have shown that a ratio of solar irradiance at the center of the Mg 280-nm doublet to that at neighboring wavelengths close to the continuum can be scaled in such a way as to reproduce variations in the irradiance ratio across the sharp change near the Al edge for the 5 years of SBUV measurements. This Mg 280-nm ratio can therefore be used to derive an empirically based representation of variations of solar ultraviolet irradiance even when the data include a time dependence that is instrumental in origin.

This empirical model shows activity-linked variations about an approximately constant level for 1979–1981, with a steady decrease in irradiance starting in late 1981. The model decrease between the 1980 average level and the level for late 1983 ranges from approximately 0.3% immediately longward of the Mg ionization edge to over 5% at 180 nm; it is nearly 4% at 204 nm, in the wavelength region that contributes to atmospheric photochemical changes. The range of average irradiance over a 27-day rotational modulation period over the 5 years is calculated to be 0.5% at 266 nm, 6% at 204 nm (the wavelength region driving atmospheric photochemistry), and 8% at 180 nm. Changes in the 27-day rotation average Mg 280-nm index measured at the SBUV band pass follow changes in 27-day average 10.7-cm radio flux well. The 10.7-cm flux can therefore be used to estimate the SBUV Mg II index ratio outside of the period of the SBUV lifetime and, by extension, variations in the solar ultraviolet. Such estimates of long-term solar variations will be valuable for studies of the relation between solar and atmospheric changes.

Acknowledgments. We thank P. K. Bhartia, R. P. Cebula, and H. Park for valuable critical scientific discussions and for making unpublished analyses of the data available to us for the preparation of the paper. The support of the Ozone Processing Team of NASA Goddard Space Flight Center in providing special data requested is gratefully acknowledged.

References

Ayres, T. R., and J. L. Linsky, The Mg II *h* and *k* lines, II, Comparison with synthesized profiles and Ca II *K*, *Astrophys. J.*, *205*, 874–894, 1976.

Brasseur, G., and S. Solomon, *Aeronomy of the Middle Atmosphere*, D. Reidel, Hingham, Mass., 1984.

Bruning, D. H., and B. J. Labonte, Interpretation of solar irradiance variations using ground-based observations, *Astrophys. J.*, *271*, 853–858, 1983.

Bumba, V., and B. Ruzickova-Topolova, Variability of integrated solar *K*-line emission, *Sol. Phys. 1*, 216–219, 1967.

Chapman, G., Active regions from the photosphere to the chromosphere, in *Solar Active Regions*, edited by F. Q. Orral, pp. 43–82, Colorado Associated University Press, Boulder, 1981.

Donnelly, R. F., D. F. Heath, and J. L. Lean, Active-region evolution and solar rotation variations in solar UV irradiance, total solar irradiance, and soft X rays, *J. Geophys. Res.*, *87*, 10,318–10,324, 1982.

Donnelly, R. F., D. F. Heath, J. L. Lean, and G. J. Rottman, Differences in the temporal variations of solar UV flux, 10.7-cm solar radio flux, sunspot number, and Ca-K plage data caused by solar rotation and active region evolution, *J. Geophys. Res.*, *88*, 9883–9888, 1983.

Fleig, A. J., D. F. Heath, K. F. Klenk, N. Oslik, K. D. Lee, H. Park, and D. Gordon, User's guide for the Solar Backscattered Ultraviolet (SBUV) and the Total Ozone Mapping Spectrometer (TOMS) RUT-S data sets: October 31, 1978 to November 1, 1980, *NASA Ref. Publ. 1112*, 1983.

Harvey, J. W., Helium 10830 Å irradiance: 1975–1983, Proceedings of Conference on Solar Irradiance Variations on Active Region Time Scales, *NASA Conf. Publ. 1210*, 1984.

Heath, D. F., A review of observational evidence for short- and long-term ultraviolet flux variability of the sun, in *Sun and Climate*, pp. 447–471, Centre National d'Etudes Spatiales, Toulouse, France, 1980.

Heath, D. F., A. J. Krueger, A. A. Roeder, and B. D. Henderson, The solar backscatter ultraviolet and total ozone mapping spectrometer for Nimbus-G, *Opt. Eng.*, *14*, 323–331, 1975.

IMSL, Inc., IMSL library reference manual, *IMSLLTB-009*, pp. RLFOR-1 to RLFOR-6, Houston, Tex., 1982.

Kjeldseth Moe, O., and Milone, E. F. Limb darkening 1945–3245 Å for the quiet sun from Skylab data, *Astrophys. J.*, *226*, 301–314, 1978.

Lean, J. L., Estimating the variability of the solar flux between 200 and 300 nm, *J. Geophys. Res.*, *89*, 1–9, 1984.

Lean, J. L., and A. Skumanich, Variability of the Lyman alpha flux with solar activity, *J. Geophys. Res.*, *88*, 5751–5759, 1983.

Lean, J. L., O. R. White, W. C. Livingston, D. F. Heath, R. F. Donnelly, and A. Skumanich, A three-component model of the variability of the solar ultraviolet flux, *J. Geophys. Res.*, *87*, 10,307–10,317, 1982.

Livingston, W., and H. Holweger, Solar luminosity variation, IV, The photospheric lines, 1976–1980, *Astrophys. J.*, *252*, 375–385, 1982.

London, J., G. G. Bjarnson, and G. J. Rottman, 18 months of UV irradiance observations from the Solar Mesospheric Explorer, *Geophys. Res. Lett.*, *11*, 54–56, 1984.

Milkey, R. W., and D. Mihalas, Resonance line transfer with partial redistribution, II, The solar Mg II lines, *Astrophys. J.*, *192*, 769–776, 1974.

Morrison, N. D., and J. L. Linsky. Photospheric models of solar active regions and the network based on the Mg II *h* and *k* line wings, *Astrophys. J.*, *222*, 723–734, 1978.

Mount, G., and G. J. Rottman, The solar absolute spectral irradiance, 1150–3173 Å: May 17, 1982, *J. Geophys. Res.*, *88*, 5403–5410, 1983*a*.

Mount, G. H., and G. J. Rottman, The solar absolute spectral irradiance at 1216 Å and 1800–3173 Å: January 12, 1983, *J. Geophys. Res.*, *88*, 6807–6811, 1983*b*.

NASA, Third and fourth year addendum to the user's guide for the solar backscattered ultraviolet (SBUV) instrument first year ozone data set, Goddard Space Flight Center, Greenbelt, Md., 1984.

National Academy of Sciences, *Solar Variability, Weather, and Climate*, National Academy Press, Washington, D. C., 1982.

Newkirk, G., Variations in solar luminosity, *Annu. Rev. Astron. Astrophys.*, *24*, 429–467, 1983.

Park, H., and D. F. Heath, Nimbus-7 SBUV/TOMS calibration for ozone measurements, in *Proceedings of The Quadrennial International Ozone Symposium, Halkidiki, Greece*, edited by C. S. Zerefos and A. Ghazi, pp. 412–416, D. Reidel, Hingham, Mass., 1985.

Rottman, G. J., 27-day variations observed in solar U.V. (120–300 nm) irradiance, *Planet. Space Sci.*, *38*, 1001–1007, 1983.

Rottman, G. J., C. Barth, R. Thomas, G. Mount, G. Lawrence, D. Rusch, R. Saunders, G. Thomas, and J. London, Solar spectral irradiance 120 nm–190 nm, October 13, 1981–January 3, 1982, *Geophys. Res. Lett.*, *9*, 587, 1982.

Simon, P. C., Solar irradiance between 120 and 400 nm and its variations, *Sol. Phys.*, *74*, 273–291, 1981.

Simon, P. C. and G. Brasseur, Photodissociation effects of UV radiation, *Planet. Space Sci.*, *31*, 987–999, 1983.

Skumanich, A. C., J. L. Lean, O. R. White, and W. C. Livingston, The sun as a star: Three-component analysis of chromospheric variability in the calcium *K* line, *Astrophys. J.*, *282*, 776–783, 1984.

Vaughan, A. H., S. L. Baliunas, F. Middelkoop, L. Hartmann, D. Mihalas, R. W. Noyes, and G. W. Preston, Stellar rotation in lower main sequence stars measured from time variations in *H* and *K* emission-line fluxes, I, Initial results, *Astrophys. J.*, *250*, 276–283, 1981.

Vernazza, J. E., E. H. Avrett, and R. Loeser, Structure of the chromosphere, II, The underlying photosphere and temperature minimum region, *Astrophys. J. Suppl. Ser. 30*, 1–60, 1976.

Wilson, O. C., Chromospheric variations in main sequence stars, *Astrophys. J.*, *226*, 379–396, 1978.

White, O. R., and W. Livingston, Solar luminosity variation, III, Calcium *K* variation from solar minimum to maximum in cycle 21, *Astrophys. J.*, *249*, 798, 1981.

D. F. Heath, Laboratory for Atmospheres, Code 963, NASA Goddard Space Flight Center, Greenbelt, MD 20771.

B. M. Schlesinger, SASC Technologies, Incorporated, 5809 Annapolis Road, Hyattsville, MD 20784.

(Received March 26, 1985;
revised February 3, 1986;
accepted February 7, 1986.)